Published in final edited form as:
Nature. 2008 May 22; 453(7194): 481–488. doi:10.1038/nature06926.

Proteasome subunit Rpn13 is a novel ubiquitin receptor

Koraljka Husnjak[1,2,7], **Suzanne Elsasser**[3,7], **Naixia Zhang**[4,7], **Xiang Chen**[4], **Leah Randles**[4], **Yuan Shi**[3], **Kay Hofmann**[5], **Kylie Walters**[4,*], **Daniel Finley**[3,*], and **Ivan Dikic**[1,2,6,*]

[1]Institute of Biochemistry II and Cluster of Excellence Macromolecular Complexes, Goethe University, Theodor-Stern-Kai 7, D-60590 Frankfurt (Main), Germany

[2]Tumor Biology Program, Mediterranean Institute for Life Sciences, Mestrovicevo setaliste, 21000 Split, Croatia

[3]Department of Cell Biology, Harvard Medical School, 200 Longwood Avenue, Boston, MA 02115, USA

[4]Department of Biochemistry, Molecular Biology and Biophysics, University of Minnesota, Minneapolis, MN 55455, USA

[5]Miltenyi Biotec GmbH, Stoeckheimer Weg 1, D-50829, Koeln, Germany

[6]Department of Immunology, Medical School University of Split, Soltanska 2, 21 000 Split, Croatia

Abstract

Proteasomal receptors that recognize ubiquitin chains attached to substrates are key mediators of selective protein degradation in eukaryotes. Here we report the identification of a new ubiquitin receptor, Rpn13/ARM1, a known component of the proteasome. Rpn13 binds ubiquitin via a conserved N-terminal region termed the Pru domain (Pleckstrin-like receptor for ubiquitin), which binds K48-linked diubiquitin with an affinity of ~90 nM. Like proteasomal ubiquitin receptor Rpn10/S5a, Rpn13 also binds ubiquitin-like domains of the UBL/UBA family of ubiquitin receptors. A synthetic phenotype results in yeast when specific mutations of the ubiquitin binding sites of Rpn10 and Rpn13 are combined, indicating functional linkage between these ubiquitin receptors. Since Rpn13 is also the proteasomal receptor for Uch37, a deubiquitinating enzyme, our findings suggest a coupling of chain recognition and disassembly at the proteasome.

In eukaryotes, selective protein degradation is performed primarily by the ubiquitin-proteasome pathway. The 26S proteasome is a huge macromolecular machine that contains a proteolytically active 20S core particle (CP) capped at one or both ends by a 19S regulatory particle (RP)1. The RP recognizes ubiquitinated substrates, deconjugates ubiquitin chains, and unfolds substrates prior to their translocation into the CP. Proteasome subunit Rpn10/S5a was shown to bind ubiquitin chains via ubiquitin-interaction motifs (UIMs)2. Receptors were subsequently identified that are not integral proteasome subunits, but deliver ubiquitinated targets to the proteasome (for reviews, see 5 and 6). Canonical members of this UBL/UBA family of receptors are Rad23 (hHR23a/b in humans), Dsk2 (hPLIC-1/2 in humans) and Ddi13,4,7-9. UBA domains bind ubiquitin[10-12] and UBL domains interact reversibly with the proteasome, principally via Rpn1, but potentially also via Rpn10[13-15].

*Correspondence: Ivan Dikic Ivan.Dikic@biochem2.de, Dan Finley daniel_finley@hms.harvard.edu, Kylie Walters walte048@umn.edu.

[7]These authors contributed equally to this work.

Accession Numbers: Coordinates for scRpn13 are available through the Protein Data Bank with accession number 2Z4D.

Another interesting component of the proteasome is Rpn13/ADRM1/ARM1[16-21], which docks at the RP *via* an N-terminal region that binds Rpn2[18,21-23]. Its C-terminal region binds deubiquitinating enzyme Uch37/UCHL5 and enhances its isopeptidase activity[18,20,21]. Uch37 may function as an editing isopeptidase that rescues poorly ubiquitinated substrates from being degraded[24].

Using a yeast two-hybrid screen, with a bait of ubiquitin lacking the last two glycines to prevent its conjugation[25], we identified the N-terminal segment of human Rpn13 (hRpn13) as a ubiquitin-binding partner. The interaction was confirmed using murine Rpn13 (mRpn13) as bait against monoubiquitin and Rpn2 as prey (Figure 1A). Rpn13 from *S. cerevisiae* (scRpn13) aligns with the ubiquitin-binding N-terminal region of hRpn13 (Figure 1B). Comprehensive sequence analysis using profiles and Hidden Markov Models failed to reveal similarity to known ubiquitin- or proteasome-binding motifs (Figure 1C and data not shown). Deletion mutants encompassing residues 1-150 were tested for tetraubiquitin binding, thus mapping the minimal binding domain to residues 1-130 (Figure 1D). Although smaller fragments of mRpn13 also showed detectable binding to ubiquitin, they were unstable and expressed poorly as GST-fusions.

The significance of the ubiquitin-Rpn13 interaction would be supported if it were conserved from yeast to mammals, particularly as budding yeast Rpn13 is truncated and the conserved N-terminal region (Figure 1C) only 25% identical to mammalian forms (Figure 1B). The existence of an unidentified ubiquitin receptor in yeast had been evident to us from the viability of a *rpn10-uim rad23*Δ *dsk2*Δ *ddi1*Δ mutant (data not shown). *rpn13*Δ mutants, which are viable but show defects in protein degradation[16,26], were used to test whether Rpn13 binds ubiquitin chains in the context of intact, purified proteasomes.

Ubiquitin chain binding by purified proteasomes can be assayed by native gel electrophoresis[3,14]. Proteasomes are visualized in this system by an activity stain, using a fluorogenic peptide substrate. For wild-type, the predominant proteasome species contains one RP on either end of the CP cylinder (RP_2CP). Ubiquitin chains, produced by the E2 enzyme Cdc34, bind to the proteasomes and confer reduced mobility (Figure 2A). This shift is not dependent on UBL-UBA proteins, since the proteasomes were prepared from *rad23Δ dsk2Δ ddi1Δ* mutants. A block substitution within the UIM in Rpn10 results in attenuation of the shift, reflecting Rpn10's known ubiquitin receptor function (Figure 2A; 3·4). However, the existence of marked residual electrophoretic retardation by added chains (lane 4) indicates the presence of at least one additional ubiquitin receptor in purified proteasomes.

Addition of conjugates to proteasomes lacking Rpn13 resulted in an electrophoretic shift comparable to that of *rpn10-uim* samples (Figure 2A). Thus, the yeast ortholog of mRpn13 is active in ubiquitin chain binding and can bind ubiquitin in the context of intact proteasomes. Indeed, its capacity for chain binding in this assay compares well with that of Rpn10. Remarkably, we observed an ostensibly complete abrogation of chain-dependent electrophoretic retardation when *rpn10-uim rpn13*Δ proteasomes were used (Figure 2A), suggesting that Rpn10 and Rpn13 are the two major ubiquitin receptors in the yeast proteasome. However, by varying the conditions of this assay, we could, as shown below, detect residual ubiquitin chain binding with *rpn10-uim rpn13*Δ proteasomes, consistent with the existence of a still unidentified proteasomal ubiquitin receptor. The greater abundance of the RP1CP and CP bands in *rpn13*Δ samples suggests that Rpn13 contributes to the stability of the RP-CP interaction *in vitro*[26].

To determine whether *rpn13Δ* proteasomes were properly assembled, they were analyzed by SDS-PAGE (Figure 2B). Apart from the absence of Rpn13 itself, the mutant proteasomes appeared to be wild-type in composition. When recombinant Rpn13 was reconstituted onto

mutant proteasomes after purification, their chain-binding defect was corrected (Figure 2C). Thus, the chain-binding assay appears to report on a specific Rpn13-ubiquitin chain interaction, and not a gross structural defect of *rpn13*Δ proteasomes. GST pull-down assays also indicated direct interaction of scRpn13 with ubiquitin (data not shown). In summary, these data indicate that Rpn13 is a novel proteasomal ubiqutin receptor.

To create mutants of scRpn13 deficient in ubiquitin binding and to subsequently study the functional significance of the interaction *in vivo*, we initially used NMR to solve the structure of full-length scRpn13. These studies revealed that Thr6-Leu101 forms two contiguous, antiparallel β-sheets with a configuration similar to the PH structural domain (Figure 3A). In particular, a β-sheet comprised of four antiparallel β-strands formed by I8-R11, E32-P37, W46-W50, and I64-L66 packs against a 3-stranded sheet formed by M74-V76, I86-V90, and R96-W100. Juxtaposed to the 3-stranded sheet are two β-strands formed by C15-N18 and L23-P26. The configuration of the β-strands centres around interactions between conserved aromatics within the protein core, including F10, F48, W50, W75, F87, F91, F98, F99, and W100. These findings are consistent with the crystal structure[27] of mRpn13. We thus named this domain Pleckstrin-like receptor for ubiquitin (Pru). In a canonical PH domain, K117-N130 of scRpn13 would be α-helical, consistent with secondary structure predictions for K119-G127. Residues S106-G127 are absent, however, from all acquired spectra, suggesting that this region undergoes conformational exchange and does not form a rigid helix. In the accompanying manuscript[27], we find that the cognate residues in mRpn13 and hRpn13 do form helices. K117-N130 of scRpn13 shares 35.7% sequence identity with mRpn13, but the presence of a glycine at position 127 likely destablizes the helix, as might substitution of the sequence QDE at the beginning of the helix with the more basic sequence KDK in scRpn13. Also, a salt bridge27 between E119 and R122 of mammalian Rpn13 is lost, as R122 is substituted with N123 in scRpn13.

To determine how scRpn13 binds ubiquitin, we performed an NMR titration series (Supplementary Figure 1), which implicated E41, E42, G44, F45, L66, E72, F91, S93 and R96 as being at the ubiquitin contact surface (Figure 3B). Interestingly, these residues are in the S2-S3, S4-S5, and S6-S7 loops (Figure 3C). The S4-S5 loop is strongly conserved in higher eukaryotes, as is F91, which is in the S6-S7 loop (Figure 1C). scRpn13 binding to monoubiquitin is in “fast exchange” by NMR, which is ideal for determining binding affinity by this method, and the affinity of scRpn13 for monoubiquitin was determined to be 65 μM (Figure 5F).

We used NMR titration experiments to determine the stoichiometry of hRpn13 for monoubiquitin, K48-linked diubiquitin, and tetraubiquitin (see Supplementary Information). Monoubiquitin and diubiquitin bound to Rpn13 with 1:1 stoichiometry, whereas two Rpn13 molecules bound one tetraubiquitin (Figure 4A and 4B). Therefore, although three potential diubiquitin elements exist within tetraubiquitin, no more than two Rpn13 molecules can be accommodated simultaneously. The exclusion of a third Rpn13 molecule is consistent with model structures of Rpn13:tetraubiquitin, in which steric clashes arise when three hRpn13 molecules bind neighbouring K48-linked ubiquitin subunits (Supplementary Figure 2). That Rpn13 binds diubiquitin elements of K48-linked chains is further validated in the accompanying manuscript[27].

In contrast to scRpn13, resonances broaden and shift as hRpn13 Pru binds monoubiquitin (Supplementary Figure 3). This behavior is associated with stronger K_d values, but prohibits their accurate calculation by the method used to determine the scRpn13:ubiquitin affinity. Fluorescence spectrophotometry was used to determine hRpn13's affinity for monoubiquitin and diubiquitin, since hRpn13 (1-150) contains two tryptophan residues and ubiquitin none. hRpn13 showed a surprisingly strong affinity, with a K_d for monoubiquitin of ~300 nM

(Figure 4C and 4D) and for diubiquitin of ~90 nM (Figure 4C and 4D). The value for diubiquitin binding is ~15-fold lower than that of hHR23a for tetraubiquitin[28]. The stronger affinity of hRpn13 for ubiquitin, as compared to scRpn13, reflects amino acid substitutions at the contact surface. For example, in the accompanying paper, residues F76 and D78 of hRpn13 were implicated in hRpn13 binding to monoubiquitin. In scRpn13, however, these residues are substituted with isoleucine and glycine, respectively.

We next analyzed whether Rpn13 exhibits specificity for ubiquitin or broadly recognizes ubiquitin family members. Using GST pull-down assays, we confirmed that ubiquitin binds to full-length mRpn13 and that this interaction requires ubiquitin's hydrophobic patch, consisting of L8, I44, and V70 (Figure 4E). mRpn13 bound more potently to linear tetraubiquitin expressed as a GST fusion (GST 4×Ub) or to purified K48-linked chains than to monoubiquitin (Figure 4E and data not shown). Under the same experimental conditions, no binding was observed between the mRpn13 Pru domain and SUMO, Nedd8, ISG15 or FAT10 (Figure 4F). In contrast, mRpn13 appeared to bind to the UBL domains of multiple UBL/UBA proteins (Supplementary Figures 4 and 5). We verified that hRpn13 Pru binds directly to the hHR23a and hPLIC2 UBL domains by NMR (Figure 4G), and determined a K_d value of 36 μM for the hRpn13 Pru:hHR23a UBL domain complex (Figure 4D and Supplementary Figure 5). Overlapping residues in hRpn13 were affected by the addition of these UBL domains (Figure 4G) or ubiquitin[27], suggesting that these interactions may be mutually exclusive.

Experiments described above implicated residues in Rpn13's S2-S3, S4-S5, and S6-S7 loops in binding ubiquitin (Figure 3). After introducing non-conservative substitutions for these residues individually or in combination, the resulting proteins were expressed in *E. coli*, purified, and characterized. We sought mutants that were defective in ubiquitin chain binding while being properly folded and proficient in proteasome binding. Separation of these functions is critical, as exemplified by previous studies of proteasomal ubiquitin receptor Rpn10. The *rpn10*Δ phenotype does not accurately reflect its function in ubiquitin recognition, because Rpn10 plays additional roles in the proteasome[4,29]. The proteasome is destabilized in the absence of Rpn10[29], as is also observed in *rpn13*Δ mutants, at least under certain *in vitro* conditions (Figure 2; 26). For Rpn13, unlike Rpn10, proteasome and ubiquitin binding are conferred by the same structural domain, and thus can be effectively separated only by precisely targeted mutations. Moreover, ubiquitin contact residues in Rpn13 are distributed over three distinct loops, and thus differ from those of Rpn10 by being non-contiguous and thus not subject to simple block mutagenesis.

We assayed Rpn13-proteasome binding by adding GST-Rpn13 to purified proteasomes. Due to the GST moiety, the fusion protein results in strong electrophoretic retardation in native gels; this effect is seen with *rpn13*Δ but not wild-type proteasomes (Figure 5A). Thus, Rpn13 assembled into the proteasome was not exchangeable with added GST-Rpn13, indicating that scRpn13 is a true proteasome subunit. Two putative ubiquitin contact site mutants of Rpn13 were demonstrated to be proficient in proteasome assembly, as shown in Figure 5B. Several other mutants failed to pass this and other preliminary assays, due typically to global folding defects (data not shown). E41 and E42 are in the S2-S3 loop, and S93 in the S6-S7 loop (Figure 5C). These sites, though greater than 22 Å apart, are both situated proximally to bound ubiquitin in a model based on the mRpn13:monoubiquitin structure[27] (Figure 5C).

To assay mutational effects on ubiquitin chain binding, we used the native gel-based assay introduced in Figure 2A. Note that the mobility shift resulting from addition of GST-Rpn13 to the proteasome (Figure 5A and 5B) is irrelevant to the chain-binding assay, since Rpn13 itself does not affect proteasome migration in gels. Only the larger GST-tagged form of

Rpn13 can do so, and, in the ubiquitin chain-binding assay, untagged Rpn13 was used. Neither the S93D mutant nor the E41K, E42K mutant conferred a strong defect in the proteasome-ubiquitin interaction, although both conferred reduced mobility shifts in comparison to wild-type Rpn13 (Figure 5D). To further impair ubiquitin binding, we combined the S2-S3 and S6-S7 mutations. The resulting protein -- a E41K, E42K, S93D triple mutant, referred to as scRpn13-KKD -- was comparable to a buffer control in its influence on the proteasome's electrophoretic mobility in the presence of ubiquitin conjugates (Figure 5E). NMR titrations revealed that scRpn13-KKD binds monoubiquitin ~8-fold more weakly than wild-type (Figure 5F; see also Supplement). To ensure that these mutations did not affect Rpn13 structural integrity, we compared a $^{1}H,^{15}N$ HSQC spectrum recorded on ^{15}N labeled scRpn13-KKD with that of wild-type (Figure 5G). Only resonances corresponding to the mutated residues or their immediate neighbors were shifted, indicating that these surface mutations did not affect Rpn13's structure. In addition, we identified the hRpn13 surface that binds Rpn2, which is remote from the substituted residues[27]. The corresponding surface in scRpn13 is preserved in Rpn13-KKD as none of the residues within it were affected. Thus, Rpn13-KKD appeared to be suitable for *in vivo* analysis of the physiological function of ubiquitin recognition by Rpn13.

To test the biological significance of the Rpn13-ubiquitin interaction, we integrated the triple mutant allele into yeast in place of the wild-type chromosomal sequence. Functional defects in proteasomes can be revealed by plate assays such as sensitivity to the arginine analog canavanine, whose incorporation into proteins causes misfolding and accelerated degradation. The enhanced substrate load is lethal to mutants lacking proper proteasome function (e.g., 3). *rpn13-KKD* mutants proved sensitive to 8 μg/ml of canavanine when in the genetic background of an *rpn10-uim* mutation (Figure 6A). Thus, the *rpn13-KKD* mutation leads to a defect in proteasome function, and interacts synthetically with another specifically targeted proteasomal ubiquitin receptor mutation. Since Rpn13 can bind UBL/UBA proteins (Figure 4G), we also investigated its genetic relationship with Dsk2 and Rad23. *rpn13-KKD* also showed a strong synthetic interaction with a null allele of proteasomal ubiquitin receptor Dsk2 (Fig. 6A). In the case of Rad23, the genetic interaction was comparatively modest. These data support the view that the docking of ubiquitin-conjugates at the proteasome via UBL/UBA proteins is not mediated obligatorily via Rpn13. In addition, binding assays performed with purified proteasomes and the UBL domains of Rad23 and Dsk2 indicate that Rpn13 is not the sole receptor for UBL/UBA proteins on the proteasome (Supplementary Figure 7). The results of the binding assays are consistent with our previous report that proteasome subunit Rpn1 binds UBL/UBA proteins[14]. Further work is required to define more precisely the extent to which Rpn13–dependent docking of ubiquitin-conjugates at the proteasome is mediated or regulated by UBL/UBA proteins.

To test whether amino acid substitutions in the ubiquitin-binding loops of Rpn13 can lead to global defects in ubiquitin metabolism, whole cell extracts from our mutants were examined by immunoblotting. High molecular weight ubiquitin conjugates, which are enriched in proteasome substrates, accumulated in the *rpn13-KKD rpn10-uim* double mutant (Fig. 6B). The defect is synthetic, as with the canavanine-sensitivity of the double mutant (Fig. 6A). We also observed an *in vivo* proteolytic defect in the *rpn13-KKD* mutant (Fig. 6C), using the model proteasome substrate Ub^{V76}-Val-$e^{\Delta K}$-ßgal[30], which was previously found to be stabilized in an *rpn13*Δ mutant[16].

Defects in proteasome assembly have been observed in *rpn13Δ* proteasomes (Figure 2; 26), and could potentially account for the phenotypes observed in Figures 6A through 6C. We therefore analyzed the assembly state of *rpn13-KKD* proteasomes by running native gels on freshly-prepared, unfractionated cell extracts[31]. We observed no significant change in level, assembly, or peptidase activity in *rpn13-KKD* proteasomes (Figure 6D). Surprisingly, no

assembly defect was observed for *rpn13Δ* proteasomes (Figure 6D). Thus, assembly defects previously observed for *rpn13Δ* proteasomes are apparently a result of *in vitro* handling.

Although the recombinant Rpn13-KKD protein is properly folded and assembled onto purified proteasomes *in vitro*, it remained possible that the mutant protein would be absent from proteasomes *in vivo* as a result of its being rapidly degraded. To assess the extent of Rpn13-KKD loading of endogenous proteasomes, we used the GST-Rpn13 add-back assay of Fig. 5A, where purified proteasomes were used. In unfractionated cell extracts, GST-Rpn13 similarly shifted *rpn13Δ* proteasomes (Figure 6E). *rpn13-KKD* proteasomes behaved as wild-type in this assay, indicating that they were fully loaded with Rpn13-KKD. We conclude that the phenotypes of the *rpn13-KKD* mutant do not reflect deficient proteasome assembly or deficient loading of Rpn13 onto proteasomes, but are specifically related to its impaired ubiquitin-binding site.

We report here the identification of a new ubiquitin receptor for the proteasome, Rpn13, which is unrelated to Rpn10 and the three UBL/UBA proteins, and moreover defines a new class of ubiquitin recognition surface. Rpn13 differs dramatically from other proteasomal ubiquitin receptors. First, whereas the UBL/UBA proteins (and perhaps Rpn10) have distinct ubiquitin and proteasome binding domains that are separated by flexible linkers, Rpn13 is docked into the proteasome via a surface that is in close spatial proximity to its ubiquitin binding region. Thus, Rpn13 may provide for a ubiquitin chain with precise positioning and polarity. Second, the UBL/UBA proteins, having a large population free of the proteasome and oftentimes multiple ubiquitin binding domains, are better equipped than Rpn13 to capture ubiquitinated substrates and then deliver them to the proteasome. Third, UBL/UBA proteins are also capable of protecting the chain during transit to the proteasome, as they inhibit deubiquitination[4,32,33]. In striking contrast, Rpn13 promotes chain deubiquitination[18,20,21]. Binding to Rpn13 both facilitates Uch37's deubiquitinating activity[20,21] and links Uch37 to the proteasome, suggesting that Rpn13 plays a major role in ubiquitin chain disassembly at the proteasome. Third, Rpn13 is exceptionally proficient at binding monoubiquitin and diubiquitin compared to other ubiquitin receptors associated with proteasome-mediated degradation. Although it is widely supposed that extended ubiquitin chains are required for degradation, contrary observations have been reported, in which monoubiquitin targets proteins to the proteasome[24,34,35]. Such substrates, although possibly rare, may be more strongly dependent on Rpn13 than those marked by chains.

Rpn13 resembles Rpn10 in its ability to bind ubiquitin-like domains of the UBL/UBA ubiquitin receptors (Figure 4D and 4G, Supplementary Figure 4 and 5), implying that Rpn13 may recruit substrates to the proteasome either directly or indirectly via UBL/UBA proteins. These observations support a hypothetical model whereby conjugates bind UBL/UBA family members, which dock them to the proteasome and pass them to the intrinsic receptors Rpn10 and Rpn13. In addition, compound complexes may be formed, in which a single conjugate is simultaneously bound by an intrinsic ubiquitin receptor and a UBL/UBA protein. Compound complexes may be favored when longer chains are delivered, leading to more stable chain-proteasome interactions, and thus more rapid substrate degradation.

Ubiquitin and the proteasome are both essential, but remarkably the inactivation of all five known proteasomal ubiquitin receptors in the same yeast strain does not appear to be lethal (data not shown). In our assays, the residual chain-binding capacity of *rpn10-uim rpn13-KKD rad23Δ dsk2Δ ddi1Δ* proteasomes is modest (Figure 5E), suggesting that the highest-affinity intrinsic receptors are now known. The unidentified receptor may be of lower affinity but comparable functionality, or it may be a receptor of typical affinity that is not intrinsic to the proteasome, such as Rad23/hHR23.

The phenotypic properties of multiply receptor deficient strains suggest functional redundancy (Figure 6; 3,32). This may reflect robustness in their principal function of delivering substrate to the proteasome. Given the number of known receptors, it is likely that docking of the chain at any of multiple locations in the proteasome will support breakdown of the target protein. However, there is apparently a deeper and more interesting functional relationship among ubiquitin receptors as well, in which they play distinct roles. For example, they have various phenotypes in isolation, albeit not lethal ones. Furthermore, proteasome function appears substantially compromised in multiply receptor-deficient strains[3,32,37]. When different receptor mutants are compared, the relative strengths of the degradation defects vary from substrate to substrate[4]. Thus, the receptors show *in vivo* specificity, although it remains unclear how specific they are and what the mechanistic basis of this specificity is. Finally, functionally redundant behavior as inferred from mutant phenotypes may not reflect the functioning of the wild-type system in a straightforward manner, since compensation can mask differentiated activities. With more detailed characterization, the individuality of proteasomal ubiquitin receptors and its mechanistic basis should become more clear.

Methods

Yeast genetics and two-hybrid screen

Standard methods were used for yeast genetics, growth assays, and protein turnover assays (see Supplementary Information). A complete list of yeast strains is in the Supplementary Information. Sequences corresponding to mouse ubiquitin lacking two terminal glycines (UbΔGG) were subcloned into pYTH9 vector[38], creating fusion proteins with the Gal4 DNA-binding domain (bait). Yeast strain Y190 was transformed with bait vector and human thymus cDNA library (Clontech) was screened as previously described38.

Antibodies and plasmids

Antibodies used were: anti-myc (9E10) and anti-Ub (P4D1) from Santa Cruz Biotechnology, anti-ADRM1 (anti-Rpn13) from Biomol, and anti-ß-galactosidase (Promega). All constructs used in this study are described in Supplementary Information.

Protein purification and biochemical assays

Recombinant proteins were expressed in and purified from Rosetta cells (Novagen). Proteasome was affinity-purified essentially as described[39]. Immunoprecipitation, immunoblotting, GST pull-down assays were performed as previously described25. Native gel analysis was performed as in 3. More detailed descriptions are available as Supplementary Information.

NMR spectroscopy

We determined the structure of full length scRpn13 as described in Supplementary Information with the data summarized in (Supplementary Table 1). Binding surfaces and affinities were determined as described in Supplementary Information.

Supplementary Material

Refer to Web version on PubMed Central for supplementary material.

Acknowledgments

We thank members of our labs, as well as D. Hoeller, G. Dittmar, J. Lipscomb and M. Schmidt, for discussions, constructive comments and critical reading of the manuscript and the UMN BMBB NMR facility and MSI BSCL.

We also thank Grzegorz Zapart for the initial Y2H ubiquitin screening, as well as Michael Groll and Patrick Schneider for allowing us to use the mRpn13:ubiquitin coordinates to generate Figure 5C. This work was supported by grants from Deutsche Forschungsgemeinschaft (DI 931/3-1), the Cluster of Excellence "Macromolecular Complexes" of the Goethe University Frankfurt (EXC115) to ID, and National Institutes of Health (CA097004 to KJW; GM043601 to DF; GM008700-CBITG to LR).

References

1. Voges D, Zwickl P, Baumeister W. The 26S proteasome: a molecular machine designed for controlled proteolysis. Annu Rev Biochem 1999;68:1015–68. [PubMed: 10872471]
2. Deveraux Q, Ustrell V, Pickart C, Rechsteiner M. A 26 S protease subunit that binds ubiquitin conjugates. J Biol Chem 1994;269:7059–61. [PubMed: 8125911]
3. Elsasser S, Chandler-Militello D, Muller B, Hanna J, Finley D. Rad23 and Rpn10 serve as alternative ubiquitin receptors for the proteasome. J Biol Chem 2004;279:26817–22. [PubMed: 15117949]
4. Verma R, Oania R, Graumann J, Deshaies RJ. Multiubiquitin chain receptors define a layer of substrate selectivity in the ubiquitin-proteasome system. Cell 2004;118:99–110. [PubMed: 15242647]
5. Elsasser S, Finley D. Delivery of ubiquitinated substrates to protein-unfolding machines. Nat Cell Biol 2005;7:742–9. [PubMed: 16056265]
6. Madura K. Rad23 and Rpn10: perennial wallflowers join the melee. Trends Biochem Sci 2004;29:637–40. [PubMed: 15544949]
7. Kleijnen MF, et al. The hPLIC proteins may provide a link between the ubiquitination machinery and the proteasome. Mol Cell 2000;6:409–19. [PubMed: 10983987]
8. Chen L, Madura K. Rad23 promotes the targeting of proteolytic substrates to the proteasome. Mol Cell Biol 2002;22:4902–13. [PubMed: 12052895]
9. Kaplun L, et al. The DNA damage-inducible UbL-UbA protein Ddi1 participates in Mec1-mediated degradation of Ho endonuclease. Mol Cell Biol 2005;25:5355–62. [PubMed: 15964793]
10. Bertolaet BL, et al. UBA domains of DNA damage-inducible proteins interact with ubiquitin. Nat Struct Biol 2001;8:417–22. [PubMed: 11323716]
11. Wilkinson CR, et al. Proteins containing the UBA domain are able to bind to multi-ubiquitin chains. Nat Cell Biol 2001;3:939–43. [PubMed: 11584278]
12. Wang Q, Goh AM, Howley PM, Walters KJ. Ubiquitin recognition by the DNA repair protein hHR23a. Biochemistry 2003;42:13529–35. [PubMed: 14621999]
13. Hiyama H, et al. Interaction of hHR23 with S5a. The ubiquitin-like domain of hHR23 mediates interaction with S5a subunit of 26 S proteasome. J Biol Chem 1999;274:28019–25. [PubMed: 10488153]
14. Elsasser S, et al. Proteasome subunit Rpn1 binds ubiquitin-like protein domains. Nat Cell Biol 2002;4:725–30. [PubMed: 12198498]
15. Walters KJ, Kleijnen MF, Goh AM, Wagner G, Howley PM. Structural studies of the interaction between ubiquitin family proteins and proteasome subunit S5a. Biochemistry 2002;41:1767–77. [PubMed: 11827521]
16. Verma R, et al. Proteasomal proteomics: identification of nucleotide-sensitive proteasome-interacting proteins by mass spectrometric analysis of affinity-purified proteasomes. Mol Biol Cell 2000;11:3425–39. [PubMed: 11029046]
17. Sone T, Saeki Y, Toh-e A, Yokosawa H. Sem1p is a novel subunit of the 26 S proteasome from Saccharomyces cerevisiae. J Biol Chem 2004;279:28807–16. [PubMed: 15117943]
18. Hamazaki J, et al. A novel proteasome interacting protein recruits the deubiquitinating enzyme UCH37 to 26S proteasomes. EMBO J 2006;25:4524–36. [PubMed: 16990800]
19. Jorgensen JP, et al. Adrm1, a putative cell adhesion regulating protein, is a novel proteasome-associated factor. J Mol Biol 2006;360:1043–52. [PubMed: 16815440]
20. Qiu XB, et al. hRpn13/ADRM1/GP110 is a novel proteasome subunit that binds the deubiquitinating enzyme, UCH37. EMBO J 2006;25:5742–53. [PubMed: 17139257]

21. Yao T, et al. Proteasome recruitment and activation of the Uch37 deubiquitinating enzyme by Adrm1. Nat Cell Biol 2006;8:994–1002. [PubMed: 16906146]
22. Ito T, et al. A comprehensive two-hybrid analysis to explore the yeast protein interactome. Proc Natl Acad Sci U S A 2001;98:4569–74. [PubMed: 11283351]
23. Gandhi TK, et al. Analysis of the human protein interactome and comparison with yeast, worm and fly interaction datasets. Nat Genet 2006;38:285–93. [PubMed: 16501559]
24. Lam YA, Xu W, DeMartino GN, Cohen RE. Editing of ubiquitin conjugates by an isopeptidase in the 26S proteasome. Nature 1997;385:737–40. [PubMed: 9034192]
25. Bienko M, et al. Ubiquitin-binding domains in Y-family polymerases regulate translesion synthesis. Science 2005;310:1821–4. [PubMed: 16357261]
26. Seong KM, Baek JH, Yu MH, Kim J. Rpn13p and Rpn14p are involved in the recognition of ubiquitinated Gcn4p by the 26S proteasome. FEBS Lett 2007;581:2567–73. [PubMed: 17499717]
27. Schreiner P, et al. Ubiquitin docking at the proteasome via a novel PH domain interaction. accompanying manuscript.
28. Raasi S, Orlov I, Fleming KG, Pickart CM. Binding of polyubiquitin chains to ubiquitin-associated (UBA) domains of HHR23A. J Mol Biol 2004;341:1367–79. [PubMed: 15321727]
29. Glickman MH, et al. A subcomplex of the proteasome regulatory particle required for ubiquitin-conjugate degradation and related to the COP9-signalosome and eIF3. Cell 1998;94:615–23. [PubMed: 9741626]
30. Johnson ES, Bartel B, Seufert W, Varshavsky A. Ubiquitin as a degradation signal. Embo J 1992;11:497–505. [PubMed: 1311250]
31. Schmidt M, Hanna J, Elsasser S, Finley D. Proteasome-associated proteins: regulation of a proteolytic machine. Biol Chem 2005;386:725–37. [PubMed: 16201867]
32. Saeki Y, Saitoh A, Toh-e A, Yokosawa H. Ubiquitin-like proteins and Rpn10 play cooperative roles in ubiquitin-dependent proteolysis. Biochem Biophys Res Commun 2002;293:986–92. [PubMed: 12051757]
33. Raasi S, Pickart CM. Rad23 ubiquitin-associated domains (UBA) inhibit 26 S proteasome-catalyzed proteolysis by sequestering lysine 48-linked polyubiquitin chains. J Biol Chem 2003;278:8951–9. [PubMed: 12643283]
34. Guterman A, Glickman MH. Complementary roles for Rpn11 and Ubp6 in deubiquitination and proteolysis by the proteasome. J Biol Chem 2004;279:1729–38. [PubMed: 14581483]
35. Boutet SC, Disatnik MH, Chan LS, Iori K, Rando TA. Regulation of pax3 by proteasomal degradation of monoubiquitinated protein in skeletal muscle progenitors. Cell 2007;130:349–62. [PubMed: 17662948]
36. Kang Y, Zhang N, Koepp DM, Walters KJ. Ubiquitin receptor proteins hHR23a and hPLIC2 interact. J Mol Biol 2007;365:1093–101. [PubMed: 17098253]
37. Elsasser S, Finley D. unpublished data.
38. Soubeyran P, Kowanetz K, Szymkiewicz I, Langdon WY, Dikic I. Cbl-CIN85-endophilin complex mediates ligand-induced downregulation of EGF receptors. Nature 2002;416:183–7. [PubMed: 11894095]
39. Leggett DS, et al. Multiple associated proteins regulate proteasome structure and function. Mol Cell 2002;10:495–507. [PubMed: 12408819]

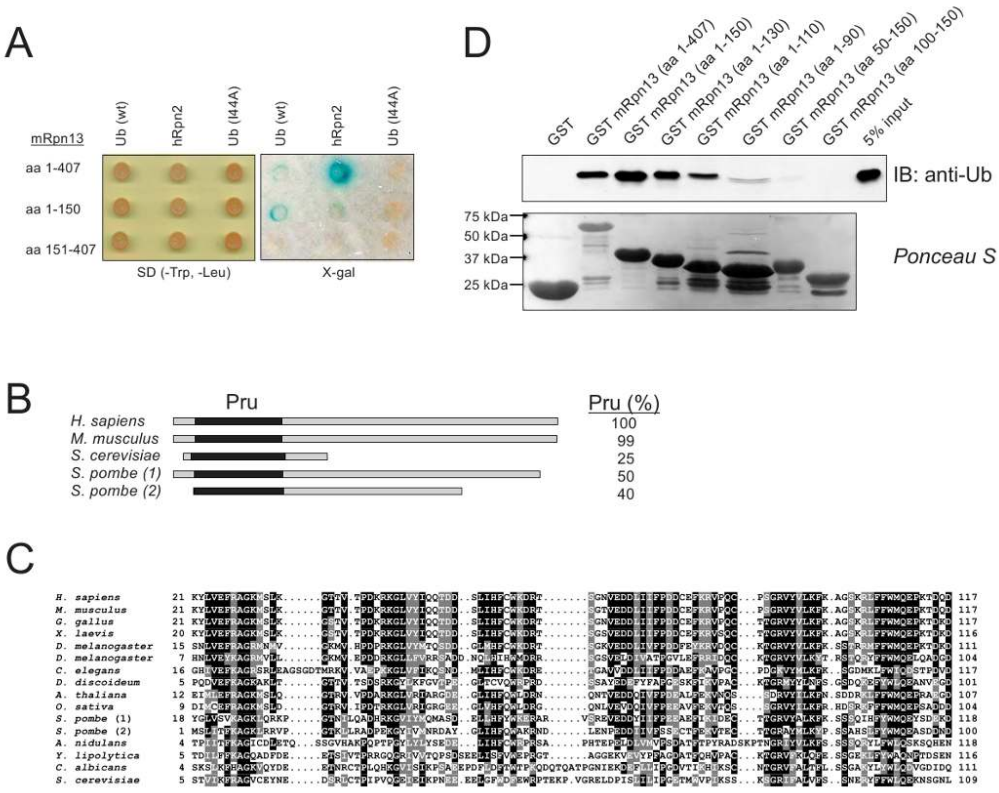

Figure 1. Murine Rpn13 binds ubiquitin chains

a, mRpn13 cDNA fragments were cloned into pYTH9 vector in frame with the Gal4 DNA-binding domain, and the resulting bait vectors transformed into yeast strain Y190 with prey pACT2 vectors containing wt-ubiquitin, I44A-ubiquitin, or hRpn2 (positive binding control) cDNA in frame with Gal4 DNA-activating domain. **b,** Architecture of Rpn13 from various species. The N-terminal domain is generally conserved (black box) whereas the C-terminal region (grey box) is absent in *S. cerevisiae* and has diverged beyond recognition in one of the two *S. pombe* proteins (*S. pombe* (1)). *S. pombe* (1)=SPCC16A11.16, *S. pombe* (2)=SPBC342.04. Percent identity to the conserved hRpn13 Pru domain is provided at right. **c**, Alignment of Rpn13 N-terminal sequences. Residues that are invariant or conserved in at least 50% of sequences are shaded in black or grey, respectively. **d**, To identify the minimal region required for ubiquitin binding, mRpn13 deletion mutants were expressed as GST-fused proteins, purified, and tested for their binding to linear tetraubiquitin by immunoblotting with anti-ubiquitin antibodies. Tetraubiquitin was obtained by thrombin cleavage of GST-fused tetraubiquitin (GST 4×Ub) and equivalent amounts of GST-fused deletion mutants were used in GST pull-down assay.

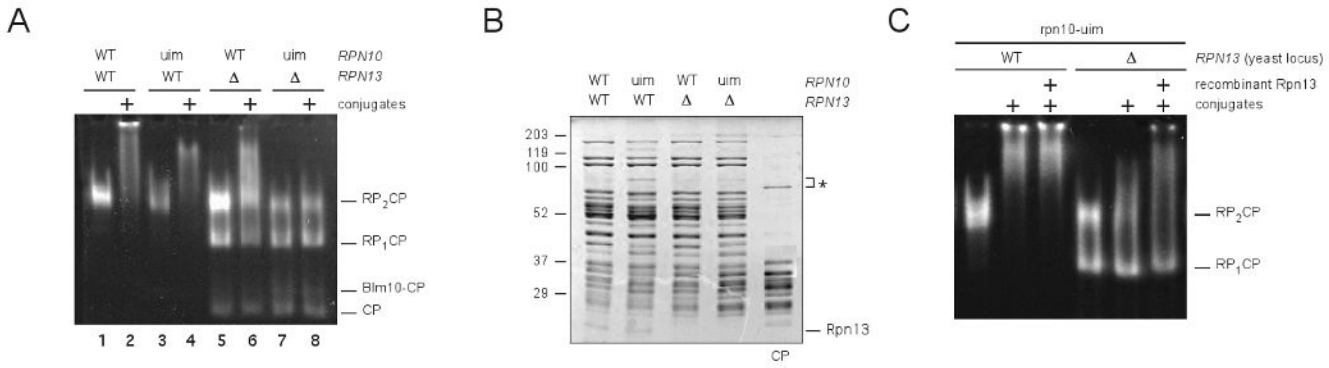

Figure 2. Rpn13 contributes to recognition of ubiquitin conjugates by the proteasome

a, *rpn13*Δ proteasomes show defects in ubiquitin conjugate binding. Proteasomes were purified from strains (SY733, SY729, SY725, and SY722) bearing the indicated mutations. Proteasomes (4 pmol) were mixed with autoubiquitinated Cdc34 (16 pmol), resolved by native PAGE, and visualized using LLVY-AMC. Note that UBL/UBA proteins cannot contribute to ubiquitin chain binding in these experiments, since all proteasomes used in this figure are from a *rad23Δ dsk2Δ ddi1Δ* genetic background. *ubp6Δ* is also in the genetic background, to prevent chain disassembly during the assay. **b**, Proteasome composition is maintained in the absence of Rpn13. Proteasomes from panel A (25 μg) were resolved by SDS-PAGE and stained with Coomassie blue. An asterisk marks contaminating protein. **c**, Reconstitution of ubiquitin conjugate binding. A subset of proteasomes from panel A (4 pmol each) was incubated with scRpn13 (20 pmol) cleaved from the GST moiety (+ lanes) or GST alone (remaining lanes) to allow reassembly, then mixed with autoubiquitinated Cdc34 (16 pmol). Complexes were resolved by native PAGE and visualized as in (A).

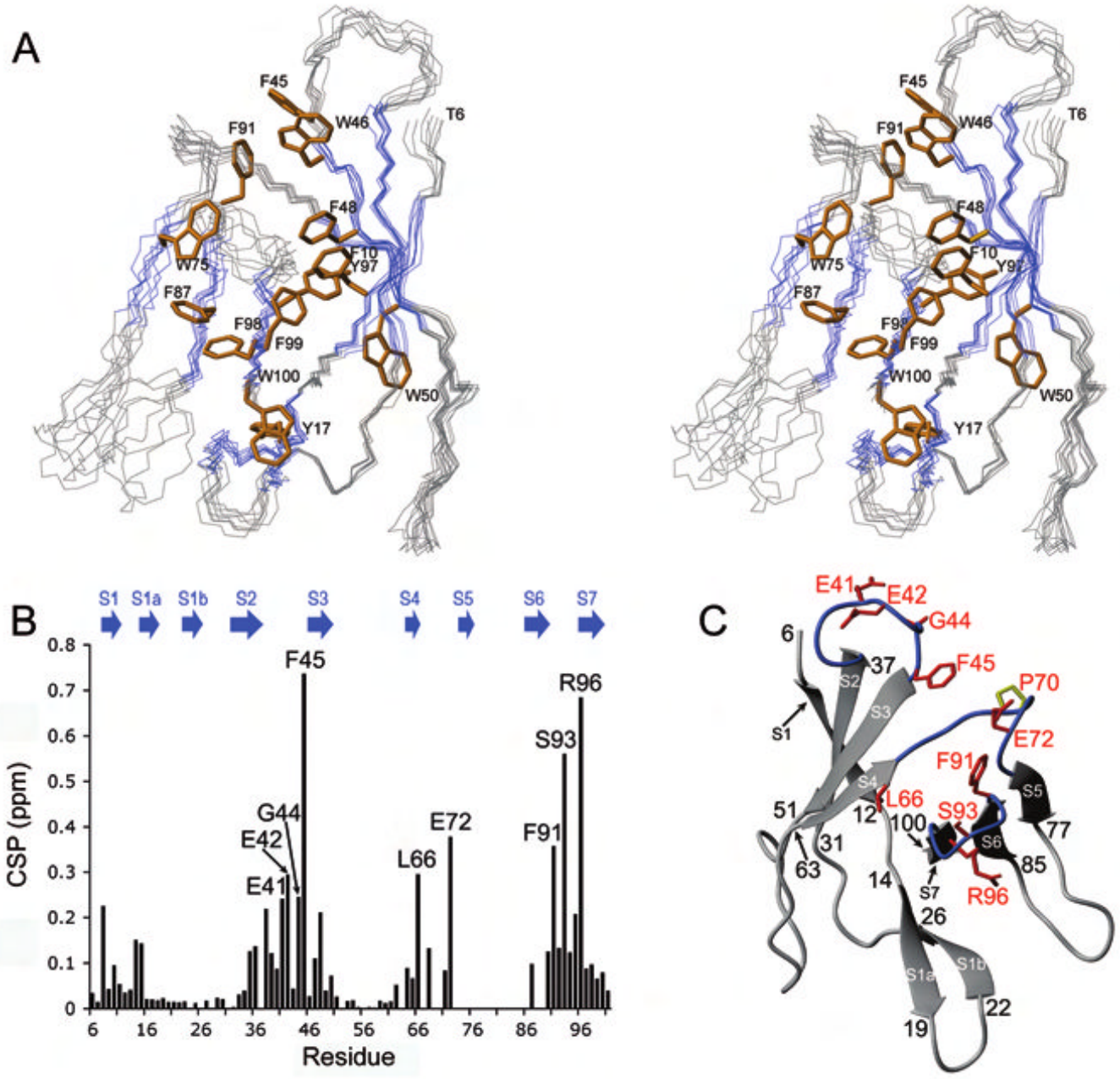

Figure 3. Rpn13 uses loops to bind ubiquitin

a, Stereoview of scRpn13, spanning residues T6-L101, in which β-strands are indicated in blue and hydrophobic sidechains in yellow. **b**, NMR titration experiments reveal scRpn13 residues that contact ubiquitin. The data were prepared as described in Methods and plotted. **c**, ScRpn13 residues that bind ubiquitin are within the S2-S3, S4-S5, and S6-S7 loops. Residues significantly affected by ubiquitin addition are displayed and labeled in red with their secondary structures in blue.

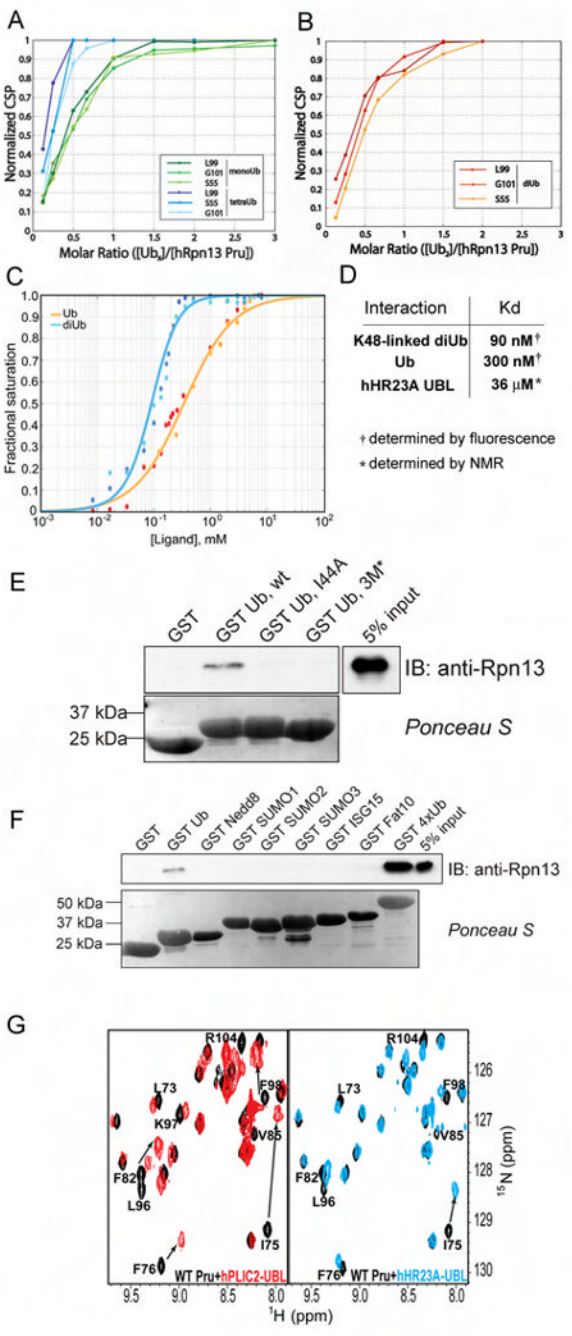

Figure 4. Rpn13 binds to ubiquitin and UBLs of proteasomal receptors

a, b, hRpn13 Pru binds K48-linked diubiquitin and monoubiquitin with 1:1 stoichiometry whereas two hRpn13 Pru molecules bind one K48-linked tetraubiquitin. Normalized chemical shift perturbation values are plotted against varying molar ratios of Rpn13 to tetraubiquitin (a, shades of blue), diubiquitin (b, shades of red), or monoubiquitin (a, shades of green) to reveal respective Rpn13:ubiquitin binding stoichiometries of 2:1, 1:1 or 1:1. Each data line represents a specific amino acid as indicated in the figure, with values determined as described in the Supplement. **c**, Binding curves for hRpn13 Pru binding to monoubiquitin or K48-linked diubiquitin as determined by intrinsic tryptophan fluorescence. Normalized fluorescence intensity values are plotted for two data sets against varying

concentration of monoubiquitin (red and orange) or diubiquitin (blue and light blue). The data were fit by assuming 1:1 binding for hRpn13 Pru and monoubiquitin (orange) or diubiquitin (light blue). **d,** Table of hRpn13 Pru binding affinities for K48-linked diubiquitin, monoubiquitin, and hHR23a's UBL domain. Values for ubiquitin binding were determined by using the fluorescence data of (c). NMR titration curves were used to determine the value for hHR23a's UBL domain. **e**, mRpn13 Pru binds to the hydrophobic patch of ubiquitin containing I44. mRpn13 Pru domain was used in GST pull-down assays to assess binding to GST-tagged monoubiquitin and its mutant derivatives (I44A and triple mutant [3M*] L8-I44-V70). **f**, mRpn13 Pru domain was used in GST pulldown assays (as in Figure 4e) to assess its binding to GST-fused ubiquitin-like protein modifiers. **g**, Rpn13 binds to the hPLIC2 and hHR23A UBL domains. ^{1}H, ^{15}N HSQC spectra of ^{15}N labeled hRpn13 Pru alone (black) and with 2-fold molar excess hPLIC2 (red) or hHR23A (blue) UBL domain indicates their direct interaction. Although the effect is greater for hPLIC2, these two UBL domains affect common residues in hRpn13 Pru, suggesting that they bind the same surface.

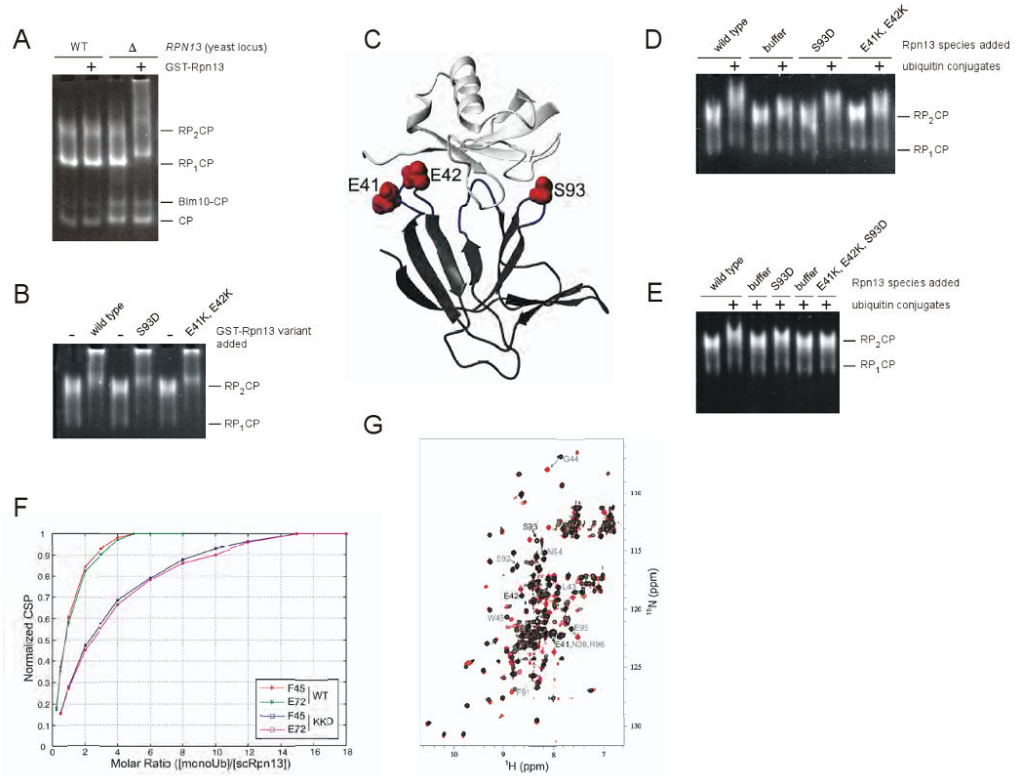

Figure 5. An Rpn13 mutant specifically defective in ubiquitin chain binding

a, Reconstitution of proteasomes with recombinant GST-Rpn13. Proteasomes were purified from strains containing or lacking Rpn13 (SY775 and SY723). GST-Rpn13 (40 pmol) or buffer was mixed with proteasomes (5 pmol), which were resolved on native PAGE and visualized using suc-LLVY-AMC. The mobility shift caused by GST-Rpn13 is an indicator of its assembly into proteasomes. The presence of GST on Rpn13 is required to cause a mobility shift. All proteasomes used in this figure are from an *rpn10-uim ubp6Δ* genetic background. **b**, Mutations in Rpn13 do not attenuate assembly of Rpn13 into the proteasome. Reconstitution assays were carried out as in panel A, but using a four-fold molar excess of GST-Rpn13. **c**, Structural model with mutations. Mutated residues (see panels D-F) were mapped onto a model structure of scRpn13 (dark grey) complexed with monoubiquitin (light grey). E41, E42 and S93 are displayed in red, ubiquitin-binding loops in blue. These residues map to the S2-S3 (E41K, E42K) and S6-S7 (S93D) loops. **d**, Mutations in single loops of Rpn13 attenuate its proteasomal ubiquitin receptor function. 12 pmol of Rpn13 variants cleaved from GST were incubated with proteasomes (3 pmol) to allow reassembly. Autoubiquitinated Cdc34 (18 pmol) was then added. After 15 min at 30°C, complexes were resolved by native PAGE and visualized using suc-LLVY-AMC. **e**, Rpn13 mutant E41K, E42K, S93D (Rpn13-KKD) abrogates the ubiquitin receptor activity of Rpn13. Experiment performed as in panel D. **f**, scRpn13-KKD affinity for monoubiquitin is significantly reduced compared to wild-type. Normalized chemical shift perturbation values are plotted against molar ratios of monoubiquitin to wild-type scRpn13 (WT, red, green) or monoubiquitin to scRpn13-KKD (KKD, blue, purple). Each data line represents a specific amino acid, namely F45 (red and blue) and E72 (green and purple). Using Matlab v. 7.2, the data were fit to determine a binding constant of 65 μM for wild-type scRpn13 and an 8-fold reduction in scRpn13-KKD's affinity for monoubiquitin. **g**, Superposition of ^{1}H, ^{15}N HSQC spectra of wild-type Rpn13 (black) and Rpn13-KKD (red). Shifted

resonances are labeled in grey and those corresponding to E41, E42 and S93 in black. Chemical shift assignments are only available for the wild-type protein.

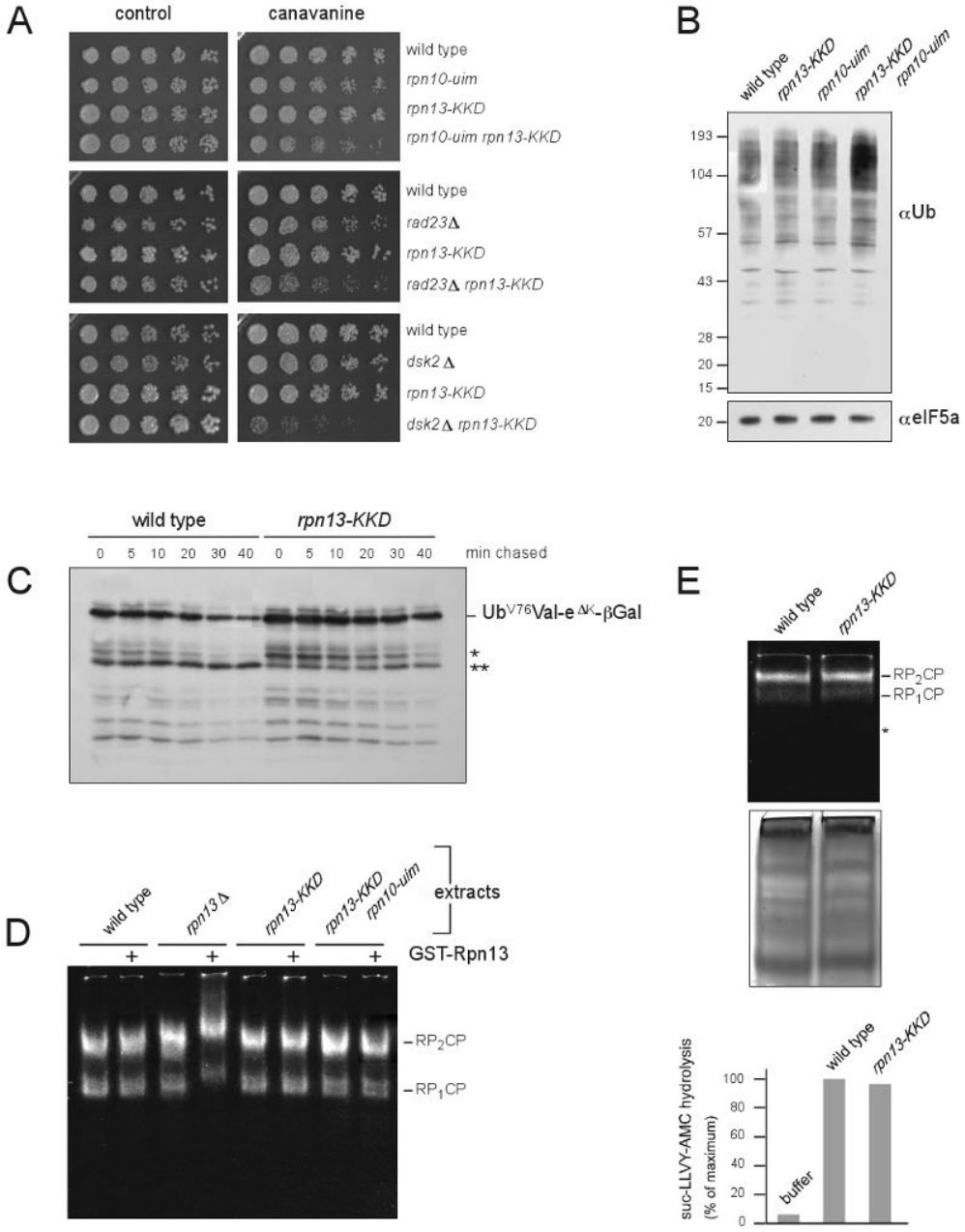

Figure 6. Phenotypic effects of the loss of ubiquitin receptor function by Rpn13

a, Canavanine sensitivity of single and double mutants in ubiquitin receptor genes. Cells in late log phase (top: SY998b, SY980f, SY1004c, and SY920b; middle: SY1076, SY1073a, SY1012a, and SY1080a; and bottom: SY1076, SY1074a, SY1012a, and SY1082a) were serially diluted and stamped on plates using a pin array. Plates were incubated at 30°C for either 2 (left) or 3 (right) days. **b**, Endogenous ubiquitin conjugate levels in proteasomal ubiquitin receptor mutants. Cells (SY998a, SY980a, SY1004a, and SY920a) were grown to log phase, and whole-cell extracts prepared. Proteins were resolved by 4-12% gradient SDS-PAGE, transferred to PVDF, and probed with antibody against ubiquitin. The membrane was stripped and probed with antibody against eIF5a. **c**, Substrate stabilization in *rpn13-*

KKD mutants. Cells (SY992b, SY1004b) expressing Ub^{V76}-Val-$e^{\Delta K}$-ßgal from a *GAL* promoter were grown to mid-log phase under inducing conditions. Protein synthesis was quenched at time zero by adding cycloheximide. Aliquots were withdrawn at the time points indicated, and lysates prepared. Proteins were visualized by SDS-PAGE/immunoblot analysis, using an antibody to ß-galactosidase, and quantified with imaging software (Kodak EDAS 290). The rate of degradation of Ub^{V76}-Val-$e^{\Delta K}$-ßgal was reduced approximately 2 fold in the *rpn13-KKD* mutant as compared with wild type. Asterisks indicate distinct ß-galactosidase-derived partial breakdown products, whose relative intensities differ between wild-type and mutant. **d**, *rpn13-KKD* mutants are not deficient in proteasome levels. Cells (SY933, SY936, SY950 and SY952) were grown to late log phase at 30°C in YPD, harvested, and lysed as described (see Supplementary Information). 150 μg of extract were resolved by native PAGE, and proteasome complexes visualized using suc-LLVY-AMC (left) and Coomassie as a loading control (middle). The asterisk indicates the expected position of the proteasome CP, which is not visualized due to low levels. Extracts were also subject to a quantitative proteasome assay, using suc-LLVY-AMC (right). **e**, Proteasomes from *rpn13-KKD* mutants are loaded with Rpn13-KKD protein. 100 μg of extract prepared for panel B was incubated with 1 μg of either GST-Rpn13 (+ lanes) or GST only (samples where GST-Rpn13 is absent) on ice. Proteasome complexes were resolved by native PAGE and visualized by suc-LLVY-AMC overlay assay.